First Demonstration of Thermally Stable Zr:HfO_2 Ferroelectrics via Inserting AlN Interlayer

Sangmok Lee, Giuk Kim, *Graduate Student Member, IEEE*, Sangho Lee, *Graduate Student Member, IEEE*, Hunbeom Shin, *Graduate Student Member, IEEE*, Youngjin Lim, Kang Kim, Do-Hyung Kim, Il-Kwon Oh, Sang-Hee Ko Park, Jinho Ahn, and Sanghun Jeon, *Senior Member, IEEE*

***Abstract*— This letter introduces a novel methodology to improve the thermal stability of Zr:HfO_2 (HZO) ferroelectric (FE) materials by adding AlN as the middle interlayer (IL) between HZO. Adding AlN to HZO improves the thermal stability of FE layers in three ways. Initially, the growth of grains and the formation of the dielectric monoclinic (m-) phase are kinetically suppressed in the HZO when subjected to a subsequent thermal budget (TB) after crystallization annealing for the formation of FE layers. The middle IL acts as a physical barrier that hinders the formation of leakage paths along grain boundaries with increasing TB. Additionally, NH_3 plasma treatment during AlN deposition improves the interface quality between the IL and bottom HZO FE layer. Collectively, these beneficial effects synergistically contribute to the enhancement of thermal stability, ensuring outstanding remanent polarization ($2P_r \approx 24\ \mu C/cm^2$) and reliability ($\approx 4.3 \times 10^4$ cycles) even under high TB (800 °C for 30 min.). This study is a significant initial step in investigating the use of HZO FE material in 3D memory devices, which require high TB due to intricate process integration.**

***Index Terms*— HfZrO, ferroelectric, hafnia, thermal stability, 3D integration, thermal budget.**

I. Introduction

HAFNIA ferroelectric (FE) materials have been actively utilized in high-performance 3D FE memory devices, thanks to their CMOS compatibility and scalability [1], [2]. Among these, the 3D FE V-NAND flash stands out as the next-generation storage memory device capable of overcoming the limitations of conventional charge trap-based NAND flash [3], [4], [5]. The switching nature of the FE, combined with charge trapping, helps achieve a large memory window and a low operation voltage in 3D FE V-NAND devices [6].

To increase the on-current of a NAND string composed of transistors connected in series, it is necessary to increase the grain size and mobility of poly-Si, which requires a high thermal budget (TB) (> 800 °C) [7], [8]. Furthermore, in order to address the decrease in electrical current resulting from the high string height in high-density V-NAND, these issues become significant. Therefore, the FE material is inevitably subjected to significantly high TB as a result of the following processes.

Accordingly, for the application of 3D FE V-NAND, it is crucial for the hafnia FE materials to ensure robust thermal stability [9]. However, unfortunately, hafnia FE layers become thermally unstable under high TB due to two origins. The first origin is the occurrence of the non-FE monoclinic (m-) phase within the FE layer under high TB conditions (Fig. 1(a)) [10], [11]. The second origin is the formation of leakage paths, resulting from increased oxygen vacancies (V_O) located along the grain boundaries in the FE layer (Fig. 1(b)) [12], [13].

Despite these challenges, research on developing thermally stable FE layers has been scarcely reported so far. Kim et al. demonstrated that adopting Al dopants, which have smaller ionic radii compared to Hf, increases both the crystallization temperature of the FE layer and the energy barrier from the tetragonal (t-) to the m-phase, providing enhanced thermal stability [14]. However, because of the nature of Al dopants, which stabilize the t-phase in the FE layer [15], a wake-up process is required to transform the t-phase to the orthorhombic (o-) phase [16], [17]. Furthermore, the narrow doping window of Al:HfO_2 hinders further performance improvement by optimizing the thickness and the Al doping concentration [18].

This letter proposes a unique method to improve the thermal stability of $Hf_{0.5}Zr_{0.5}O_2$ (HZO) material by adding AlN as an interlayer (IL) within the FE layer. HZO is extensively researched thanks to its broad doping window and sufficient remanent polarization ($2P_r$) property even in the pristine state [19], [20]. The AlN IL within the HZO film suppresses the unwanted m-phase stabilization (Fig. 1(c)) and inhibits the formation of continuous grain boundaries, therefore preventing the creation of leakage routes (Fig. 1(d)). The NH_3 plasma treatment enhances the interfacial quality of HZO during AlN deposition, which improves its polarization switching behavior and leakage current properties, as shown in Fig. 1(e). We provide an in-depth discussion of our experimental findings that

Manuscript received 9 June 2024; accepted 3 July 2024. Date of publication 11 July 2024; date of current version 27 August 2024. This work was supported in part by the Technology Innovation Program (TIP) under Grant RS-2023-00231985, Grant RS-2023-00235655, and Grant RS-2024-00406007; and in part by the Ministry of Science and ICT (MSIT) under Grant RS-2023-00260527. The review of this letter was arranged by Editor A. I. Khan. *(Sangmok Lee and Giuk Kim contributed equally to this work.) (Corresponding authors: Jinho Ahn; Sanghun Jeon.)*

Sangmok Lee, Giuk Kim, Sangho Lee, Hunbeom Shin, and Sanghun Jeon are with the School of Electrical Engineering, Korea Advanced Institute of Science and Technology (KAIST), Daejeon 34141, South Korea (e-mail: jeonsh@kaist.ac.kr).

Youngjin Lim and Il-Kwon Oh are with the Division of Electrical and Computer Engineering, Ajou University, Suwon 16499, South Korea.

Kang Kim, Do-Hyung Kim, and Sang-Hee Ko Park are with the School of Materials Science and Engineering, Korea Advanced Institute of Science and Technology (KAIST), Daejeon 34141, South Korea.

Jinho Ahn is with the Division of Materials Science and Engineering, Hanyang University, Seoul 04763, South Korea (e-mail: jhahn@hanyang.ac.kr).

Color versions of one or more figures in this letter are available at https://doi.org/10.1109/LED.2024.3424973.

Digital Object Identifier 10.1109/LED.2024.3424973

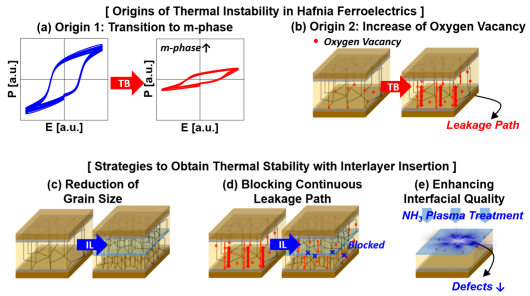

Fig. 1. Schematics of the origins of thermal instability in hafnia FE and the effects of AlN IL insertion on thermal stability. (a) Stabilization of non-FE m-phase and (b) increase of V_O with increasing TB. (c) First effect of inserting IL (AlN): suppression of m-phase through reduction of grain size. (d) Second effect: reduced leakage current by blocking the grain boundaries, where V_O migrate. (e) Third effect: the NH3 plasma treatment during deposition of AlN IL to enhance interfacial quality.

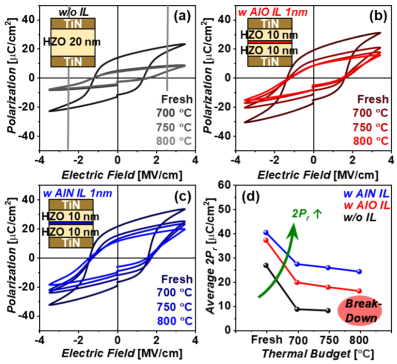

Fig. 2. Pristine P-E curves for MFM devices with various stacks: (a) HZO without IL, (b) HZO with AlO IL, and (c) HZO with AlN IL. (d) Variations of $2P_r$ with respect to the TB.

show how our method improves the thermal stability of the HZO layer. We successfully developed a thermally stable HZO film with a $2P_r$ of approximately 24 $\mu C/cm^2$ and endurance of around 4.3×10^4 cycles, even after being subjected to a TB of 800 °C for 30 minutes. Our study presents a practical method of producing thermally stable hafnia FE materials suitable for 3D FE V-NAND memory applications, which demand high TB due to intricate process integration.

II. Experimental Section

We conducted an experiment to assess the impact of AlN middle IL on thermal stability using metal-FE-metal (MFM) devices as outlined in Fig. 2(a)-(c). The lower electrodes made of TiN (100 nm) were deposited using DC sputtering. Subsequently, HZO, AlO, and AlN IL were deposited using plasma-enhanced atomic layer deposition (PEALD), utilizing TEMAHf, TEMAZr, and TMA as precursors, respectively. The 1 nm-thick AlO and AlN interfacial layers were formed through the utilization of O_2 and NH_3 plasma. The use of NH_3 plasma during AlN deposition naturally incorporates NH_3 plasma treatment. TiN top electrodes (1nm) were deposited using PEALD, utilizing $TiCl_4$ and NH_3 plasma as precursor and reactant, respectively. Afterward, Ti/Pt (10/50 nm) electrodes were deposited by an electron beam evaporation system. Finally, RTA process was conducted at 600 °C for 10 sec. For testing TB, fresh devices were subjected to furnace annealing at temperatures of 700 °C, 750 °C, and 800 °C for 30 min.

III. Results and Discussion

Fig. 2(a)-(c) depict the pristine P-E hysteresis curves for MFM devices with various stacks as a function of TB.

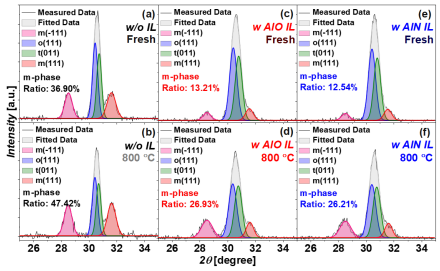

Fig. 3. Deconvoluted GIXRD spectra with respect to TB. (a)-(b) HZO without IL, (c)-(d) HZO with AlO IL, and (e)-(f) HZO with AlN IL.

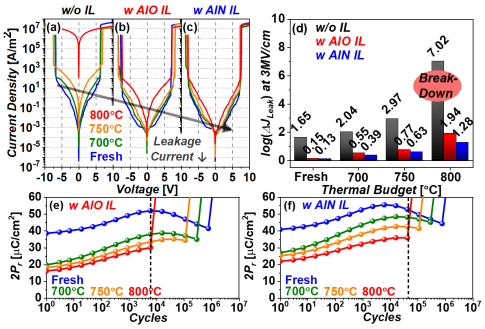

Fig. 4. Measured I-V characteristics of (a) MFM devices without intermediate IL, with (b) AlO and (c) AlN IL. (d) Compared increase of leakage current of devices with respect to TB. (e)-(f) Endurance characteristics of MFM capacitors with AlO and AlN IL.

Fig. 2(d) shows the $2P_r$ in relation to the TB. The results highlight the beneficial impact of including AlN as an insertion IL between HZO layers. For device without IL, a significant decrease in FE properties was observed with increasing TB, indicating a transformation from the metastable t-phase to the irreversible m-phase under high TB. Introducing IL significantly reduced the deterioration of FE characteristics, even after being exposed to TB at 800 °C for 30 minutes. The introduction of the intermediate IL within the HZO layers hindered grain growth, resulting in a higher surface-to-volume ratio and thus preventing the formation of the unwanted m-phase [21], [22], [23]. Fig. 3(a)-(f) displays deconvoluted GIXRD spectra, suggesting the effect of IL on phase transition. To analyze the ratio of each phase, diffraction peaks of m(−111), o(111), t(011), and m(111) were set at 28.54, 30.4, 30.8, and 31.64 degrees, respectively [21]. Devices without IL exhibited significant m-phase emergence with respect to thermal budget. In contrast, for the devices with IL, the m-phase evolution is hindered. Meanwhile, devices without IL were electrically broken down during thermal testing at 800°C for 30 minutes, while devices with IL did not. This indicates that ILs prevent the formation of continuous grain boundaries that could lead to leakage paths along the grain boundaries [22], [24]. Those containing AlN as an intermediate IL exhibited improved FE characteristics ($2P_r \approx 24\ \mu C/cm^2$) in comparison to those with AlO IL ($2P_r \approx 16\ \mu C/cm^2$). The NH_3 plasma treatment during the AlN IL deposition improved polarization by suppressing the formation of defects such as V_O at the IL/bottom HZO interface.

An investigation was conducted to quantify the suppression effect of V_O-induced leakage paths by inserting an AlN IL. The evaluation was focused on the features of the leakage current. Fig. 4(a)-(c) show the current-voltage (I-V) curves for three different stacks (HZO, HZO with AlO, and HZO with AlN) with TB. Fig. 4(d) depicts the results of applying

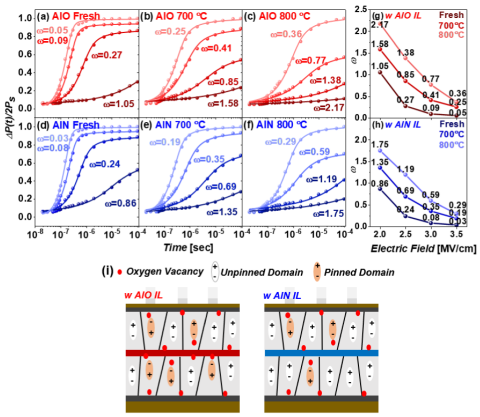

Fig. 5. (a)-(f) Time-dependent polarization switching properties and (g)-(h) half-width-half-maximum (ω) of Lorentzian distribution function of MFM devices with AlO and AlN ILs with TB. (i) Schematics of domain pinning effects due to V_O in AlO and AlN IL inserted device.

the logarithm to the increase in leakage current (I_{Leak}) values under an external electric field of 3 MV/cm. HZO without an IL typically exhibits high leakage current, which significantly worsens as the annealing temperature increases. On the other hand, HZO with IL exhibits minimal leakage current, and a decrease in leakage current with higher TB was noted, suggesting that the insertion of ILs efficiently inhibits the creation of leakage paths. In addition, inserting AlN improves FE characteristics and decreases leakage current. The device with AlN IL shows enhanced performance in leakage current compared to the capacitor with AlO IL, particularly evident at a TB of 800 °C for 30 minutes. The endurance properties of MFM devices with various IL types in relation to TB (Fig. 4(e)-(f)) also suggest the impact of AlN IL insertion. Subjecting the device to a TB of 800 °C for 30 minutes showed that the device with the AlO IL had poor endurance, but the capacitor with the AlN IL showed improved endurance. The improved properties and endurance characteristics of the FE stem from the AlN IL introduction, which benefits from both AlN's intrinsic features and NH_3 plasma treatment during deposition. The nature of AlN makes it resistant to diffusion from neighboring layers and less likely to readily accept foreign atoms. Peng et al. found that nitrogen atoms close to the HZO hinder the diffusion of Hf/Zr during annealing [25]. Similarly, Kim et al. presented that metal nitrides effectively functions as a diffusion barrier to adjacent layers [26]. Regarding NH_3 plasma treatment, the extra surface treatment during AlN deposition helps reduce the occurrence of defects, representatively V_O, leading to an improved surface quality between HZO and AlN [27]. Chen et al. showed that treating the HZO layer with NH3 plasma results in the creation of a $HfZrO_xN_y$ passivation layer on the HZO surface, which helps decrease V_O formation in subsequent processes [28]. In addition, research on the mechanism underlying the decrease in V_O after NH_3 plasma treatment on HZO surfaces has been consistently reported [29], [30]. Wu et al. found that N-bonding hinders oxygen displacement on the surface of HZO and reduces the formation of V_O [30]. NH_3 plasma treatment has been shown to improve the quality of interfaces by passivating dangling bonds and decreasing interface traps in materials like HZO and others [25], [31], [32]. However, V_O reduction caused by NH_3 plasma treatment does not significantly affect the wake-up effect because the effect is limited to the interface.

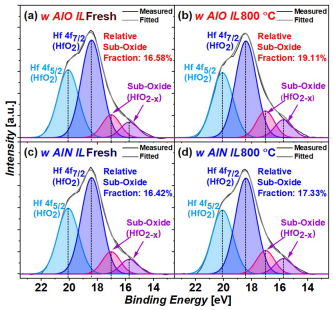

Fig. 6. Deconvoluted XPS Hf 4f spectra of IL/Bottom HZO interface with respect to TB. (a)-(b) HZO with AlO IL, and (c)-(d) HZO with AlN IL.

Fig. 5(a)-(f) show the time-dependent polarization switching properties ($\Delta P/Ps$) of MFM devices with AlO and AlN IL, respectively. The data was analyzed with the nucleation-limited switching (NLS) model, which included the Lorentzian distribution [33]. When comparing the HZO with AlO IL, the FE layer with AlN IL shows sharper switching and lower half-width-half-maximum (ω) at all TB conditions (Fig. 5(g)-(h)). This indicates that FE domain switching mainly happens at particular external electric field and pulse periods, indicating a large domain size. The improved FE switching characteristics were enhanced by NH_3 plasma treatment, preventing V_O production that causes domain pinning effect as shown in Fig. 5(i) [16]. Fig. 6(a)-(d) depicts deconvoluted XPS Hf 4f spectra at the IL/bottom HZO interface. To consider spin-orbital splitting for Hf 4f spectra, peaks for HfO_2 were assigned at 18.41 and 20.08eV, while the peaks for sub-oxide were assigned at 15.72 and 17.02 eV, in agreement with published data [34]. It can be verified that relative fraction of sub-oxides, which are indicative of V_O formation, is suppressed in device with AlN IL, especially in high TB condition.

IV. Conclusion

This research showcases the enhanced thermal stability of a HZO layer by the use of AlN as an intermediate IL. Through rigorous experimental investigation, we have identified three impacts of the AlN IL that successfully reduce the thermal instability in HZO FE layers. Stabilization of non-FE m-phase and formation of leakage channels along grain boundaries are prevented. Consequently, we achieved outstanding FE and lower leakage characteristics even after exposure to high TB. Furthermore, enhancing the interface quality with NH_3 plasma treatment improves FE qualities and reduces leakage current. We developed a thermally stable HZO film with exceptional qualities, maintaining a remanent polarization of approximately 24 $\mu C/cm^2$ and enduring around 4.3×10^4 cycles even after exposure to a TB of 800 °C for 30 minutes. Our research results aid in developing thermally stable FE HZO layers, allowing for their use in 3D FE V-NAND devices.

References

[1] M. Jung, V. Gaddam, and S. Jeon, "A review on morphotropic phase boundary in fluorite-structure Hafnia towards DRAM technology," *Nano Converg.*, vol. 9, no. 1, Oct. 2022, Art. no. 44, doi: 10.1186/s40580-022-00333-7.

[2] M. Kobayashi, J. Wu, Y. Sawabe, S. Takuya, and T. Hiramoto, "Mesoscopic-scale grain formation in HfO_2-based ferroelectric thin films and its impact on electrical characteristics," *Nano Converg.*, vol. 9, no. 1, Nov. 2022, Art. no. 50, doi: 10.1186/s40580-022-00342-6.

[3] G. Kim, S. Lee, T. Eom, T. Kim, M. Jung, H. Shin, Y. Jeong, M. Kang, and S. Jeon, "High performance ferroelectric field-effect transistors for large memory-window, high-reliability, high-speed 3D vertical NAND flash memory," *J. Mater. Chem. C*, vol. 10, no. 26, pp. 9802–9812, 2022, doi: 10.1039/d2tc01608g.

[4] K. Florent, M. Pesic, A. Subirats, K. Banerjee, S. Lavizzari, A. Arreghini, L. Di Piazza, G. Potoms, F. Sebaai, S. R. C. McMitchell, M. Popovici, G. Groeseneken, and J. Van Houdt, "Vertical ferroelectric HfO_2 FET based on 3-D NAND architecture: Towards dense low-power memory," in *IEDM Tech. Dig.*, Dec. 2018, pp. 2.5.1–2.5.4, doi: 10.1109/IEDM.2018.8614710.

[5] G. Kim, T. Kim, S. Lee, J. Hwang, M. Jung, J. Ahn, and S. Jeon, "Novel strategies for low-voltage NAND flash memory with negative capacitance effect," *Jpn. J. Appl. Phys.*, vol. 63, no. 5, May 2024, Art. no. 05SP06, doi: 10.35848/1347-4065/ad3f23.

[6] E. J. Shin, G. Lee, S. Kim, J. H. Chu, and B. J. Cho, "Dual-mechanism memory combining charge trapping and polarization switching for wide memory window flash cell," *IEEE Electron Device Lett.*, vol. 44, no. 7, pp. 1108–1111, Jul. 2023, doi: 10.1109/LED.2023.3282366.

[7] J. Akhtar, S. K. Lamichhane, and P. Sen, "Thermal-induced normal grain growth mechanism in LPCVD polysilicon film," *Mater. Sci. Semiconductor Process.*, vol. 8, no. 4, pp. 476–482, Aug. 2005, doi: 10.1016/j.mssp.2004.10.003.

[8] S.-Y. Kim, J. K. Park, W. S. Hwang, S.-J. Lee, K.-H. Lee, S. H. Pyi, and B. J. Cho, "Dependence of grain size on the performance of a polysilicon channel TFT for 3D NAND flash memory," *J. Nanoscience Nanotechnol.*, vol. 16, no. 5, pp. 5044–5048, May 2016, doi: 10.1166/jnn.2016.12251.

[9] I. Kim and J. Lee, "Dopant engineering of Hafnia-based ferroelectrics for long data retention and high thermal stability," *Small*, vol. 20, no. 13, Nov. 2023, Art. no. 2306871, doi: 10.1002/smll.202306871.

[10] M. Hoffmann, U. Schroeder, T. Schenk, T. Shimizu, H. Funakubo, O. Sakata, D. Pohl, M. Drescher, C. Adelmann, and R. Materlik, "Stabilizing the ferroelectric phase in doped hafnium oxide," *J. Appl. Phys.*, vol. 118, no. 7, Aug. 2015, Art. no. 072006, doi: 10.1063/1.4927805.

[11] M. Park, Y. Lee, T. Mikolajick, U. Schroeder, and C. Hwang, "Thermodynamic and kinetic origins of ferroelectricity in fluorite structure oxides," *Adv. Electron. Mater.*, vol. 5, no. 3, Dec. 2018, Art. no. 1800522, doi: 10.1002/aelm.201800522.

[12] M. Pešić, F. P. G. Fengler, L. Larcher, A. Padovani, T. Schenk, E. D. Grimley, X. Sang, J. M. LeBeau, S. Slesazeck, U. Schroeder, and T. Mikolajick, "Physical mechanisms behind the field-cycling behavior of HfO_2-based ferroelectric capacitors," *Adv. Funct. Mater.*, vol. 26, no. 25, pp. 4601–4612, May 2016, doi: 10.1002/adfm.201600590.

[13] K. Florent, A. Subirats, S. Lavizzari, R. Degraeve, U. Celano, B. Kaczer, L. Di Piazza, M. Popovici, G. Groeseneken, and J. Van Houdt, "Investigation of the endurance of FE-HfO_2 devices by means of TDDB studies," in *Proc. Annu. Int. Symp. Rel. Phys.*, 2018, pp. 6D.3-1–6D.3-7, doi: 10.1109/IRPS.2018.8353634.

[14] G. Kim, H. Shin, T. Eom, M. Jung, T. Kim, S. Lee, M. Kim, Y. Jeong, J.-S. Kim, and K.-J. Nam, "Design guidelines of thermally stable Hafnia ferroelectrics for the fabrication of 3D memory devices," in *IEDM Tech. Dig.*, Dec. 2022, pp. 5.4.1–5.4.4, doi: 10.1109/IEDM45625.2022.10019458.

[15] C.-K. Lee, E. Cho, H.-S. Lee, C. S. Hwang, and S. Han, "First-principles study on doping and phase stability of HfO_2," *Phys. Rev. B, Condens. Matter*, vol. 78, no. 1, Jul. 2008, Art. no. 012102, doi: 10.1103/physrevb.78.012102.

[16] H. J. Kim, M. H. Park, Y. J. Kim, Y. H. Lee, T. Moon, K. D. Kim, S. D. Hyun, and C. S. Hwang, "A study on the wake-up effect of ferroelectric $Hf_{0.5}Zr_{0.5}O_2$ films by pulse-switching measurement," *Nanoscale*, vol. 8, no. 3, pp. 1383–1389, Oct. 2016, doi: 10.1039/c5nr05339k.

[17] T.-J. Chang, H.-Y. Chen, C.-I. Wang, H.-C. Lin, C.-F. Hsu, J.-F. Wang, C.-H. Nien, C.-S. Chang, I. P. Radu, and M.-J. Chen, "Wake-up-free ferroelectric $Hf_{0.5}Zr_{0.5}O_2$ thin films characterized by precession electron diffraction," *Acta Mater.*, vol. 246, Mar. 2023, Art. no. 118707, doi: 10.1016/j.actamat.2023.118707.

[18] Y. Choi, J. Shin, S. Moon, J. Min, C. Han, and C. Shin, "Experimental study of endurance characteristics of al-doped HfO_2 ferroelectric capacitor," *Nanotechnology*, vol. 34, no. 18, Feb. 2023, Art. no. 185203, doi: 10.1088/1361-6528/acb7fc.

[19] A. H.-T. Nguyen, M.-C. Nguyen, A.-D. Nguyen, J.-Y. Yim, J.-H. Kim, N.-H. Park, S.-J. Jeon, D. Kwon, and R. Choi, "Impact of Pt grain size on ferroelectric properties of zirconium hafnium oxide by chemical solution deposition," *Nano Converg.*, vol. 9, no. 1, Oct. 2022, Art. no. 45, doi: 10.1186/s40580-022-00334-6.

[20] M. H. Park, H. J. Kim, Y. J. Kim, Y. H. Lee, T. Moon, K. D. Kim, S. D. Hyun, F. Fengler, U. Schroeder, and C. S. Hwang, "Effect of Zr content on the wake-up effect in $Hf_{1-x}Zr_xO_2$ films," *ACS Appl. Mater. Interfaces*, vol. 8, no. 24, pp. 15466–15475, Jun. 2016, doi: 10.1021/acsami.6b03586.

[21] M. Park, H. Kim, Y. Kim, W. Lee, T. Moon, and C. Hwang, "Evolution of phases and ferroelectric properties of thin $Hf_{0.5}Zr_{0.5}O_2$ films according to the thickness and annealing temperature," *Appl. Phys. Lett.*, vol. 102, no. 24, Jun. 2013, Art. no. 242905, doi: 10.1063/1.4811483.

[22] H. Kim, M. Park, Y. Kim, Y. Lee, W. Jeon, T. Gwon, T. Moon, K. Kim, and C. Hwang, "Grain size engineering for ferroelectric $Hf_{0.5}Zr_{0.5}O_2$ films by an insertion of Al_2O_3 interlayer," *Appl. Phys. Lett.*, vol. 105, no. 19, Nov. 2014, Art. no. 192903, doi: 10.1063/1.4902072.

[23] M. Lederer, K. Seidel, R. Olivo, T. Kämpfe, and L. M. Eng, "Effect of Al_2O_3 interlayers on the microstructure and electrical response of ferroelectric doped HfO_2 thin films," *Frontiers Nanotechnol.*, vol. 4, p. 58, Aug. 2022, doi: 10.3389/fnano.2022.900379.

[24] Y. Xu, Y. Yang, S. Zhao, T. Gong, P. Jiang, S. Lv, H. Yu, P. Yuan, Z. Dang, Y. Ding, Y. Wang, Y. Chen, Y. Wang, J. Bi, and Q. Luo, "Robust breakdown reliability and improved endurance in $Hf_{0.5}Zr_{0.5}O_2$ ferroelectric using grain boundary interruption," *IEEE Trans. Electron Devices*, vol. 69, no. 1, pp. 430–433, Jan. 2022, doi: 10.1109/TED.2021.3126283.

[25] H. Peng, C. Chan, K. Chen, and Y. Wu, "Enabling large memory window and high reliability for FeFET memory by integrating AlON interfacial layer," *Appl. Phys. Lett.*, vol. 118, no. 10, Mar. 2021, Art. no. 103503, doi: 10.1063/5.0036824.

[26] M. Kim, Y. Goh, J. Hwang, and S. Jeon, "Enabling large ferroelectricity and excellent reliability for ultra-thin hafnia-based ferroelectrics with a w bottom electrode by inserting a metal-nitride diffusion barrier," *Appl. Phys. Lett.*, vol. 119, no. 26, Dec. 2021, Art. no. 262905, doi: 10.1063/5.0072692.

[27] D.-R. Hsieh, C.-C. Lee, T.-C. Hong, W.-J. Yeh, and T.-S. Chao, "Reliability of multiple-layer stacked gate-all-around poly-Si nanosheet channel ferroelectric HfxZr$_{1-x}$O$_2$FETs with NH_3 plasma treatment," *IEEE Trans. Electron Devices*, vol. 70, no. 7, pp. 3915–3920, Jul. 2023, doi: 10.1109/TED.2023.3274610.

[28] K.-Y. Chen, P.-H. Chen, R.-W. Kao, Y.-X. Lin, and Y.-H. Wu, "Impact of plasma treatment on reliability performance for $HfZrO_x$-based metal-ferroelectric-metal capacitors," *IEEE Electron Device Lett.*, vol. 39, no. 1, pp. 87–90, Jan. 2018, doi: 10.1109/LED.2017.2771390.

[29] Y. Lin, C. Teng, C. Hu, C. Su, and Y. Tseng, "Impacts of surface nitridation on crystalline ferroelectric phase of $Hf_{1-x}Zr_xO_2$ and ferroelectric FET performance," *Appl. Phys. Lett.*, vol. 119, no. 19, Nov. 2021, Art. no. 192102, doi: 10.1063/5.0062475.

[30] C.-H. Wu, J. Liu, X.-T. Zheng, Y.-M. Tseng, M. Kobayashi, V. P.-H. Hu, and C.-J. Su, "Robust recovery scheme for MFIS-FeFETs at optimal timing with prolonged endurance: Fast-unipolar pulsing (100 ns), nearly zero memory window loss (0.02 %), and self-tracking circuit design," in *IEDM Tech. Dig.*, Dec. 2023, pp. 1–4, doi: 10.1109/IEDM45741.2023.10413819.

[31] K. Sardashti, K. Hu, K. Tang, S. Madisetti, P. McIntyre, S. Oktyabrsky, S. Siddiqui, B. Sahu, N. Yoshida, and J. Kachian, "Nitride passivation of the interface between high-k dielectrics and SiGe," *Appl. Phys. Lett.*, vol. 108, no. 1, Jan. 2016, Art. no. 011604, doi: 10.1063/1.4939460.

[32] H.-K. Peng, C.-M. Liu, Y.-C. Kao, P.-J. Wu, and Y.-H. Wu, "Improved immunity to sub-cycling induced instability for triple-level cell ferroelectric FET memory by depositing $HfZrO_x$ On NH_3 plasma-treated Si," *IEEE Electron Device Lett.*, vol. 43, no. 8, pp. 1219–1222, Aug. 2022, doi: 10.1109/LED.2022.3185000.

[33] W. Wei, W. Zhang, L. Tai, G. Zhao, P. Sang, Q. Wang, F. Chen, M. Tang, Y. Feng, and X. Zhan, "In-depth understanding of polarization switching kinetics in polycrystalline $Hf_{0.5}Zr_{0.5}O_2$ ferroelectric thin film: A transition from NLS to KAI," in *IEDM Tech. Dig.*, 2021, pp. 19.1.1–19.1.4, doi: 10.1109/IEDM19574.2021.9720664.

[34] A. S. Sokolov, Y.-R. Jeon, S. Kim, B. Ku, D. Lim, H. Han, M. G. Chae, J. Lee, B. G. Ha, and C. Choi, "Influence of oxygen vacancies in ALD HfO_{2-x} thin films on non-volatile resistive switching phenomena with a Ti/HfO_{2-x}/Pt structure," *Appl. Surf. Sci.*, vol. 434, pp. 822–830, Mar. 2018, doi: 10.1016/j.apsusc.2017.11.016.